https://doi.org/10.5194/wes-2020-34
Preprint. Discussion started: 17 March 2020

eawe european academy of wind energy
Open Access WIND ENERGY SCIENCE DISCUSSIONS

Grid-forming control strategies for blackstart by offshore wind farms

Anubhav Jain[1], Jayachandra N. Sakamuri[2], and Nicolaos A. Cutululis[1]

[1]DTU Wind Energy, Technical University of Denmark, 4000 Roskilde, Denmark
[2]Vattenfall A/S, 6000 Kolding, Denmark

Correspondence: Anubhav Jain (anub@dtu.dk)

Abstract. Large-scale integration of renewable energy sources with power-electronic converters is pushing the power system closer to its dynamic stability limit. This has increased the risk of wide-area blackouts. Thus, the changing generation profile in the power system necessitates the use of alternate sources of energy such as wind power plants, to provide blackstart services in the future. This however, requires *grid-forming* and not the traditionally prevalent *grid-following* wind turbines. In this paper, four different grid-forming control strategies have been implemented in an HVDC-connected wind farm. A simulation study has been carried out to test the different control schemes for the different stages of energization of onshore load by the wind farm. Their transient behaviour during transformer inrush, converter pre-charge and de-blocking, and onshore block-load pickup, has been compared to demonstrate the blackstart capabilities of grid-forming wind power plants for early participation in power system restoration.

1 Nomenclature

AB	Auxiliary Breaker
AVC	AC Voltage Control
AVR	Automatic Voltage Regulator
BS	Black Start
BSU	Black Start Unit
CLC	Current Limitation Control
DPC	Direct Power Control
dPLL	Distributed PLL-based (control)
DR	Diode Rectifier
ESS	Energy Storage System
GSC	Grid Side Converter
HVAC	High Voltage Alternating Current
HVDC	High Voltage Direct Current

https://doi.org/10.5194/wes-2020-34
Preprint. Discussion started: 17 March 2020

eawe european academy of wind energy
Open Access WIND ENERGY SCIENCE DISCUSSIONS

LVRT	Low Voltage Ride Through
MB	Main Breaker
MMC	Modular Multi-level Converter
OWF	Offshore Wind Farm
PCC	Point of Common Coupling
PEC	Power Electronic Converter
PIR	Pre Insertion Resistor
PIT	Pre Insertion Time
PLL	Phase Locked Loop
PSC	Power Synchronization Control
PSL	Power Synchronization Loop
RES	Renewable Energy System
RHP	Right Half Plane
RSC	Rotor Side Converter
SG	Synchronous Generator
SM	Synchronous Machine
SVG	Synchronous Var Generator
TOV	Temporary Over Voltage
TSO	Transmission System Operator
VSC	Voltage Source Converter
VSG	Virtual Synchronous Generator (control)
WPP	Wind Power Plant
WT	Wind Turbine
WT-DC	Wind Turbine (PEC-interface) DC link

2 Introduction

Environmental problems like global warming, coupled with increasing fuel prices and the global drive towards sustainable development & energy security, has accelerated the integration of renewable energy sources (RES) into power systems all around the world. Many countries have set out several energy strategies for a more secure, sustainable and low-carbon economy like the European Union's (EU) 2018 directive on the promotion of the use of energy from renewable sources (RED II) that sets an overall goal across the EU for a 32% share of RES in the total energy consumption by 2030. Such aims and measures to also exploit the potential of RES in transport and district-heating & cooling sectors, shows huge promise for electricity as the *fuel*

https://doi.org/10.5194/wes-2020-34
Preprint. Discussion started: 17 March 2020

eawe european academy of wind energy
Open Access WIND ENERGY SCIENCE DISCUSSIONS

of the future. Among the different RES, wind energy has seen a rapid growth in the installed capacity worldwide, from about 6.1 GW in 1996 to about 591.5 GW in 2018 (Tavner, 2012) and shows a huge promise for the future to be a major electricity source.

High volume integration of RES into the power system makes it harder to maintain reliability and stability of power supply in the grid due to introduction of variable power flows and thus complicating grid operation (De Boeck et al., 2016). Moreover, the decrease in reactive power reserve due to replacement of conventional synchronous generation destabilizes the long-distance transmission corridors between load-centres and large-scale RES, such as offshore wind farms (OWF), during system contingencies (Sarkar et al., 2018). Additionally, inertial decoupling from the grid by the power electronic converter (PEC) interface with over-burdened reserves results in decreased transient stability. This increases the risk of wide-area blackouts, especially in strongly linked networks (De Boeck et al., 2016). For example, as per the report by Australian Energy Market Operator, the failure of wind farm owners to comply with performance requirements to ride through major disruptions and disturbances led to blackout of the South Australia system in 2017, that affected about 850,000 people causing disruption to households, businesses, transport & community services, and major industries. Another very recent case is the unexpected reduction of 737 MW from Hornsea 1 OWF in the UK, that is cited to be one of the main causes of the system failure in August 2019 affecting about 1 million customers and causing travel chaos in and around London, according to the technical report by National Grid (2019a).

2.1 The changing paradigm

Traditionally, blackstart (BS) service has been provided mainly by coal or gas-fired generators and pumped hydro storage due to their capability to meet all the technical requirements (Elia, 2018; National Grid, 2019b). However, due to the previously mentioned decarbonisation aims, rising fuel costs coupled with ageing assets and reducing load factors, large conventional generation plants are being phased out in favour of renewables and non-traditional technologies which increases the cost of *warming-up* large generators and thus blackstart services (National Grid, 2019b). Since maintaining the status quo for blackstart & restoration is not an option, considerable changes are required to facilitate the participation of alternate sources like RES and non-traditional technologies in the BS-market given the modern evolving energy landscape. According to Elia (2018), there is a potential to open up the delivery of BS-service to aggregation of units (combined services) including variable generation (like wind, solar-PV), especially with support from energy storage systems (ESS). National Grid has also recently confirmed that combined services, interconnectors and sites with trip to houseload can also potentially provide BS-services.

Blackstart and islanding operation requirements have been included as options for wind power plants (WPP) in the ENTSO-E network codes, where the relevant TSO is allowed to request these functions to support grid-recovery (Göksu et al., 2017). Driven by grid codes, state-of-the-art wind turbines (WT) are already capable of providing *some* services that are a part of the restoration process eg. frequency control (Fast Frequency Response) & voltage support (Low Voltage Ride Through, LVRT), and are expected to deliver more advanced requirements like Inertia Emulation, Power Oscillation Damping and Reactive Current Injection, which are increasingly being demanded by grid-codes (Jain et al., 2019). This is possible due to the advanced functionalities of the full-scale PEC interface of modern WTs, mentioned in Chen et al. (2009), like improved

https://doi.org/10.5194/wes-2020-34
Preprint. Discussion started: 17 March 2020

eawe european academy of wind energy
Open Access WIND ENERGY SCIENCE DISCUSSIONS

LVRT, self-commutation capabilities and independent control of active P & reactive Q/(Var) power. Seca et al. (2013) show that WTs owing to their fast start-up/ramp-up times, can be included earlier in the restoration process to provide Var-support and pickup load, thus decreasing the impact of a blackout event by reducing the restoration time & unserved load. However, connection of the currently prevalent *grid-following* WTs in the beginning of the restoration procedure can cause a recurrence of blackout as the grid connection is generally not stable enough (El-Zonkoly, 2015).

2.2 Wind for blackstart

Large OWFs can provide fast & fully-controlled, high-power, emission-free *green* blackstart services but there exists a gap between the present grid-code BS-requirements and current WT BS-capabilities as identified by Jain et al. (2019). Technological changes are neeeded to make WTs *BS-ready/BS-able* and the technical challenges associated with the different stages of energisation of an HVDC-connected OWF, along with control techniques to mitigate those issues have been discussed by Jain et al. (2018). A recent report by National Grid (2019b) also summarises the technological capability of non-traditional technologies like renewables & distributed energy sources to provide blackstart & restoration services. As regards wind power, large OWFs with full-scale converters and connected at the transmission level have the potential to meet the huge Var-requirements of network energisation (mainly long cables & lines), withstand transformer inrush transients, and cater to block loading, *provided* sufficient wind is available *and* controllers are adapted for blackstart. This makes HVDC transmission preferable for future OWFs due to the large charging Var required for long distance HVAC cables (Erlich et al., 2013).

The current turbine & converter controls are designed assuming a strong grid connection point which means that the grid-side converter (GSC) of the WT latches onto a pre-existing voltage signal provided by the onshore grid in case of an AC-connected OWF, or produced by the offshore HVDC converter operating in voltage-frequency control mode in case of HVDC-connected OWF (Bahrman and Bjorklund, 2014). However, to allow outward-energisation of the network of inter-array cables & transformers, create a power island that can supply local loads and energize the HVDC link converters & export cable with the ultimate aim to supply onshore block load, the WT should be able to produce its own voltage signal. This requires grid-*forming*, traditionally referred to as *voltage*-injecting control, as opposed to the conventional grid-*following* or *current*-injecting control. The two control philosophies are very well explained by (Rocabert et al., 2012). Voltage-injecting control concepts have been shown to deliver a superior performance compared to their current-injecting counterparts in system-split scenarios as demonstrated by Heising et al. (2019). Erlich et al. (2017) also shows that the temporary over-voltages (TOV) following islanding due to transformer-cable interaction can be avoided. Moreover, grid-forming WTs can also minimize the use of diesel generators that are currently employed to supply backup auxiliary power required for energization. Although, most modern WTs have an on-board UPS to power communications, protection & control for few hours during emergency shutdown (Göksu et al., 2017), a larger internal backup supply would be required for self-starting the WT for blackstart, especially after extended shutdown periods.

https://doi.org/10.5194/wes-2020-34
Preprint. Discussion started: 17 March 2020

eawe european academy of wind energy
Open Access WIND ENERGY SCIENCE DISCUSSIONS

2.2.1 Hybrid

Traditional current-controlled WTs can be used with an external power supply (eg. diesel generator/energy storage) and a Synchronous Var Generator (SVG) or STATCOM, combining services into a joint *hybrid* blackstart unit (BSU) to facilitate WT participation in BS procedure as proposed in Aktarujjaman et al. (2006). The external supply provides startup power and sets the reference voltage & frequency for the isolated system, the SVG/STATCOM supports the Var requirement of the cables & transformers and stabilizes the voltage, after which the WTs connect to meet the load power demand. Zhu et al. (2018) shows that earlier participation of WT in the restoration procedure is feasible as grid-forming control allows blackstart & stand-alone island operation with better inherent *synchronous-machine like* inertial response during a transient, that can help absorb the initial impact of energization and ensure smooth load pickup, thus mitigating large voltage/frequency excursions that might occur during restoration. However, only the transients during load pickup and re-synchronisation to the grid have been studied, while energization of collector lines, export cables & transformers, that cause more transient stability challenges during energization, are not shown. Additionally, the major energization transients are taken by the ESS & SVG, while the WTs behave as *passive* power-sources to meet load-demand during the last stages of restoration.

2.2.2 HVAC

Recent studies by Martínez-Turégano et al. (2018) and Aten et al. (2019) demonstrate the potential capability of HVAC-connected OWFs to blackstart onshore grid using grid-forming controls in less than 25% WTs *and* assuming adequate wind resource. The results show that it is possible to do *sequential* energization of the array-cables & WT transformers, starting with one WT energizing its string followed by others synchronizing to it and then sharing the control of voltage & frequency. Shorter cable sections are energized first until enough WTs are connected to absorb the Var generated by subsequent cable sections. However, according to Elia (2018) & National Grid (2019b), a large gap to bridge is the energization of the export link while meeting grid code requirements.

2.2.3 HVDC

HVDC with Voltage Source Converters (VSC) can also be used as a standby facility for blackstart and restoration of the onshore AC grid, as demonstrated by the excellent voltage and frequency control performance in real system tests done by Jiang-Hafner et al. (2008), proving for the first time that VSC-HVDC helps reduce restoration time while facilitating a safer & smoother restoration process with lower investment & maintenance cost. With HVDC transmission gaining momentum as the preferred choice for longer distance connections to larger OWFs, Sørensen et al. (2019) show that the Skagerrak-4 (SK4) VSC-HVDC link between Norway & Denmark (DK) can be successfully used to ramp-up the voltage of an islanded 400 kV & 150 kV DK-network to energize overhead transmission lines, transformers and block load, followed by synchronisation to continental EU. Additionally, a *top-down* restoration test of the NEMO link between Belgium & the UK also demonstrates the capability of the VSC-HVDC interconnector to energize a *dead* Belgian grid from the *live* UK side (Schyvens, 2019). However, a diesel generator was used to provide auxiliary power for the *dead*-side converter. Simulation results by Becker et al. (2017)

https://doi.org/10.5194/wes-2020-34
Preprint. Discussion started: 17 March 2020

eawe european academy of wind energy
Open Access WIND ENERGY SCIENCE DISCUSSIONS

show, without any details of the transformer/cable energization transients, that a VSC-HVDC connected OWF can respond to onshore load changes and participate in load restoration. Cai et al. (2017) analyzes the inrush current of transformers and cables (HVAC/HVDC) using EMT simulations, but with a diesel generator to pre-charge the offshore converter that then energizes the offshore collector grid, and the onshore converter pre-charged from onshore AC-grid, contrary to what is expected from an OWF to provide blackstart service. Simulation results presented by Sakamuri et al. (2019) demonstrate, for the first time, an HVDC-connected OWF with grid-forming control, sequentially energizing the offshore AC network including transformer, cables & converter through a pre-insertion resistor, followed by HVDC link energization and onshore converter pre-charging & de-blocking for picking up block load, successfully participating in restoration as a BSU. However, the energy imbalance in the HVDC link during the *DC-side* uncontrolled pre-charging of the onshore converter leads to a significant dip in HVDC voltage and large transients in the offshore & onshore converter cell voltages & valve currents. Grid-forming control, in addition to enabling blackstart and islanding capabilities of WTs, can also allow the use of *Hybrid*-HVDC connection with a diode rectifier unit (DRU) instead of the offshore VSC. The application of controls proposed in Blasco-Gimenez et al. (2010) for an OWF to ramp up the offshore AC grid voltage & control frequency, considering it as an inverter-based microgrid, has shown improved steady-state regulation during islanding when the DR-HVDC is not conducting, and smooth transition to current-control during grid-connected operation. This significantly reduces the cost-vs-performance, due to lower losses, especially for higher power levels, and lesser capital cost, along with increasing efficiency & reliability due to a lower probability of commutation failure than a VSC (Andersen and Xu, 2004).

2.3

This paper attempts to provide a generalized structure of different grid-forming control strategies that can be applied for controlling wind turbines as voltage sources to enable the blackstart and islanding capabilities of offshore wind farms. It then focuses on testing four different methods during the various stages of energization of an onshore block-load by an HVDC-connected OWF. The aim is to characterize the different techniques and compare their capability to deal with the transients in a controlled manner while maintaining stable voltage and frequency at the offshore terminal.

3 Grid Forming

Grid forming control of power electronic converters has been well studied for microgrids, where the role of PECs is to act as an interface between the small-scale distributed/renewable power generation units and the consumption points, leading to intertial decoupling of the rotating machines and making the microgrid system susceptible to oscillations caused by network disturbances. Grid forming allows a PEC to mimic Synchronous Generators (SG) for droop-based load-sharing, *synthetic* inertial-emulation, synchronized & stand-alone operation and blackstart behaviour, ensuring voltage and frequency stablility in *low-inertia* microgrids during varying loads, network disturbances and system configurational changes (islanding $\Longleftrightarrow$ grid-connected) (Tayyebi et al., 2018).

https://doi.org/10.5194/wes-2020-34
Preprint. Discussion started: 17 March 2020

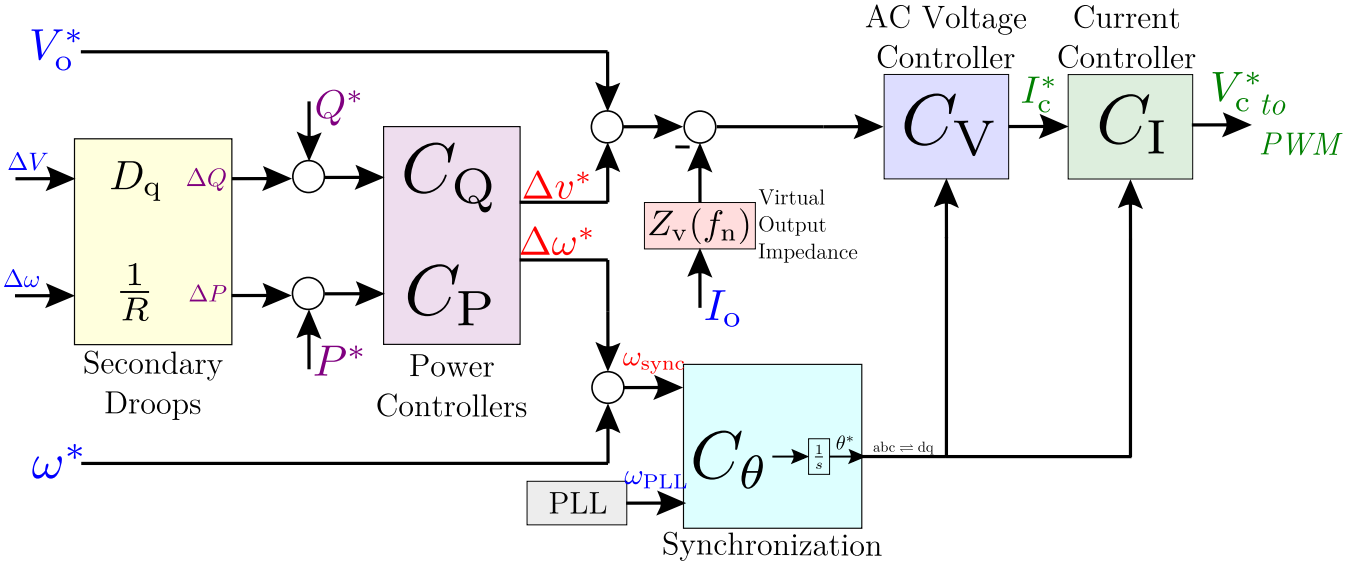

Figure 1. Grid forming control structure consisting of: inner current control loop C_{I}, the main AC voltage controller C_{V}, outer real & reactive power control loops $C_{\mathrm{P,Q}}$ and secondary droops (eg. virtual governor $\frac{1}{R}$ & virtual AVR D_{q}). Harmonic dependent virtual output impedance $Z_{\mathrm{v}}(f_{\mathrm{n}})$ can also be added.

An OWF is like a microgrid rich in power electronics although very different in that the voltage and power levels are much higher. Moreover, wind farm operators maintain a large amount (>100s) of WT-assets that are located very far from each other. Current sharing techniques for low rated inverters like the centralized controllers and the master-slave approach can be used only for paralleled systems that are close to each other and interconnected through high-bandwidth communication channels (Rocabert et al., 2012). These communication-based solutions can *not* be used for microgrids spread across several kilometres, as ensuring globally available, bidirectional, reliable & robust, low-power secure communication architecture becomes increasingly costly. Moreover, larger communication links increase delays which is undesirable in cases where a fast high-bandwidth link is required. This gave way to *droop control* algorithms with a *hierarchical* structure being used in microgrids, especially for islanded operation of many micro-sources located far away from each other (Pogaku et al., 2007). Although rated at much lower power, these grid-forming droop-based strategies can be extended to large power OWFs operating in islanded mode, *taking into account their characteristcs*, as demonstrated by Blasco-Gimenez et al. (2010).

3.1 Control Structure

According to the definition in Rocabert et al. (2012), grid-*forming* converters are controlled in closed loop to work as ideal AC voltage sources (low-output impedance), while grid-*feeding/following* converters are controlled as current sources with high parallel output impedance and can't operate in islanding/stand-alone mode as they require a grid-forming converter or local SG to set the bus voltage and frequency.

https://doi.org/10.5194/wes-2020-34
Preprint. Discussion started: 17 March 2020

eawe european academy of wind energy
Open Access WIND ENERGY SCIENCE DISCUSSIONS

The control structure of grid-forming control consists of different functional blocks, as shown in figure 1. Since the main objective of grid forming control is to operate the PEC as an ideal AC voltage source of given amplitude V_o^* and frequency ω^*, it consists most importantly of a *voltage* control loop C_{V}. The short-comings of the *single-loop* approach, explained in Zeni et al. (2015), are already known from switch-mode power supplies and electrical machine drives as over-currents during transients & faults can not be limited due to the lack of an explicit closed-loop current controller. In addition, sensitivity to disturbances and plant-parameter fluctuations eliminates *open-loop* control as a good choice. The most commonly used alternative thus, is the *nested/cascaded* voltage-current controller (Zeni et al., 2015), in which a *faster* inner *current* control loop C_{I} is added. C_{I} is designed to have a relatively smaller time constant than C_{V}, for decoupling i.e. C_{I} behaves as an almost perfect current controller for the slower C_{V}. The controllers are in the synchronous reference frame that uses an angle θ^* (for $abc \rightleftharpoons dq$ transformation) obtained from the *synchronization* block (Green and Prodanović, 2007).

While grid-feeding converters require perfect synchronism with the AC voltage at the point of connection to accurately regulate the power exchange with the grid, in the case of grid-forming converters the synchronization system must provide precise signals for *both* islanded and grid-connected modes of operation. It works as a fixed frequency ω^* *oscillator* in the former case while slowly varies the phase-angle & frequency of the island voltage during the reconnection transient to resynchronize with the grid voltage, in the latter. The most extended method used is a Phase Locked Loop (PLL), also called *voltage-based* synchronization as the frequency and phase-angle of the grid voltage vector is used for control. However, enhancements are needed to ensure stability under unbalanced and distorted voltage conditions as voltage sag, weak grids or off-grid operation can lead to instabilities. Alterately, *power-based* synchronization can also be used for synchronization as the structure of the *swing equation* that governs synchronous machine (SM) dynamics, can be equated to that of a PLL, in the sense that the PLL structure can be modified to extract the derivative term of the frequency (inertia in SMs) and the speed variation (damping in SMs), as shown in van Wesenbeeck et al. (2009). This presents a more stable solution and allows the power controller to also act as the synchronization block.

The outer *power* control loops $C_{\mathrm{P}}, C_{\mathrm{Q}}$ are required to regulate the real P and reactive Q powers exchanged with the grid (in grid-connected mode) or meet the demand set by the load (in islanded mode), while ensuring communication-less real & reactive power sharing between the multiple paralleled inverters. The simplest method for this, by only relying on local measurements, is the *droop control* scheme, which was initially introduced for SGs in utility scale grids, and now is well incorporated into microgrids (Arbab-Zavar et al., 2019). The primary level of the *3-level hierarchical* control, explained in Guerrero et al. (2011), employs droop control equations 1 & 2, based on grid X/R ratio, to mimic the self-regulation capability of a grid-connected SG and allow power sharing in microgrids without using critical communication links (Rocabert et al., 2012).

$$\text{X»R: } \omega = \omega^* - k_{\mathrm{P}}^{\omega}(P - P^*) \text{ and } V = V^* - k_{\mathrm{Q}}^{V}(Q - Q^*) \tag{1}$$

$$\text{X«R: } \omega = \omega^* + k_{\mathrm{Q}}^{\omega}(Q - Q^*) \text{ and } V = V^* - k_{\mathrm{P}}^{V}(P - P^*) \tag{2}$$

https://doi.org/10.5194/wes-2020-34
Preprint. Discussion started: 17 March 2020

eawe european academy of wind energy
Open Access WIND ENERGY SCIENCE DISCUSSIONS

Although easy to implement with high reliability and flexibility, traditional droop control suffers from an inherent tradeoff between load-sharing & voltage-regulation, load dependent frequency-deviation, slow dynamic response due to filters for P, Q and non-linear load-sharing issues due to harmonics. A variable *virtual impedance* Z_{V} can be used to add harmonic (f_{n}) droop characteristics and improve tradeoff between current harmonic sharing & voltage total harmonic distortion, by adjusting output impedance seen by harmonics and the fundamental. Additionally, this allows intelligent mode-switching with soft-start to take advantage of the fast converter response while avoiding large transients (Guerrero et al., 2011). Instead of the traditional P-f droop control, the swing equation governing SM dynamics with inertia and damping, can also be used to have a steady-state $\frac{\Delta P}{\Delta f}|_{\infty}$ droop characteristic, as shown by the equivalence of the two in D'Arco and Suul (2013). Finally, the swing equation controller, essentially a low pass filter, can be replaced by enhanced electromechanical controller dynamics (eg. detailed SM emulation, or PI & Lead-Lag (LL) controllers) to remove the inherent limitations of SMs and provide adjustable characteristics like independent tuning of inertia, damping & steady-state droop (using LL), or high non-linear behaviour during grid faults and connection/disconnection processes. However, in case of no steady-state droop (for PI) or damping-constrained droop (for swing equation), external *secondary* droops need to be added, like virtual governor droop R for real power sharing and virtual Automatic Voltage Regulator (AVR) for reactive power sharing between the paralleled PEC-interfaced WTs.

3.2 Control Strategies

In the last decade, many different control solutions have been proposed in literature to replicate the system-level functionalities of SGs like intertial & damping characteristics, frequency/voltage droop, self-organising parallel operation and automatic power sharing. The VIrtual Synchronous MAchine (VISMA) concept, introduced by Beck and Hesse (2007), uses a power-based synchronization method with a detailed implementation of the electro-mechanical model of a SM in its power control loop, thus eliminating the need for PLL and allowing conventional and proven grid operation with the usual static and dynamic properties that are characteristic to SMs, both desired *and undesired*. Since a virtual rotating mass is created which is electrically effective in relation to the grid, VISMA makes it possible to connect every kind of distributed micro-sources and renewables even to weak grids. Many improvements have been made based on the VISMA concept, as listed in D'Arco and Suul (2013), including Reduced order SM model for easier implementation and to avoid unnecessary details, Synchronverter (Zhong and Weiss, 2009) for mimicing only the *static* behaviour of SG using swing equation & reactive power control for the excitation voltage. Parallely, the Virtual Synchronous Generator (VSG) concept (van Wesenbeeck et al., 2009) emulates the swing equation by using the structure of PLL for power-synchronization. Additional enhancements include virtual impedance/admittance, damping correction loop, PLL removal (Qing-Chang Zhong et al., 2014), and virtual governor & AVR based loops. Recently, non-linear control based grid-forming strategies relying on duality between PEC & SM have been proposed like SM-matching (Arghir et al., 2018) and Virtual Oscillator Control (Johnson et al., 2017), that provide steady-state droop-like behaviour with a faster & better damped response during transients. The four grid-forming control strategies, that have been selected for this study, are explained ahead.

https://doi.org/10.5194/wes-2020-34
Preprint. Discussion started: 17 March 2020

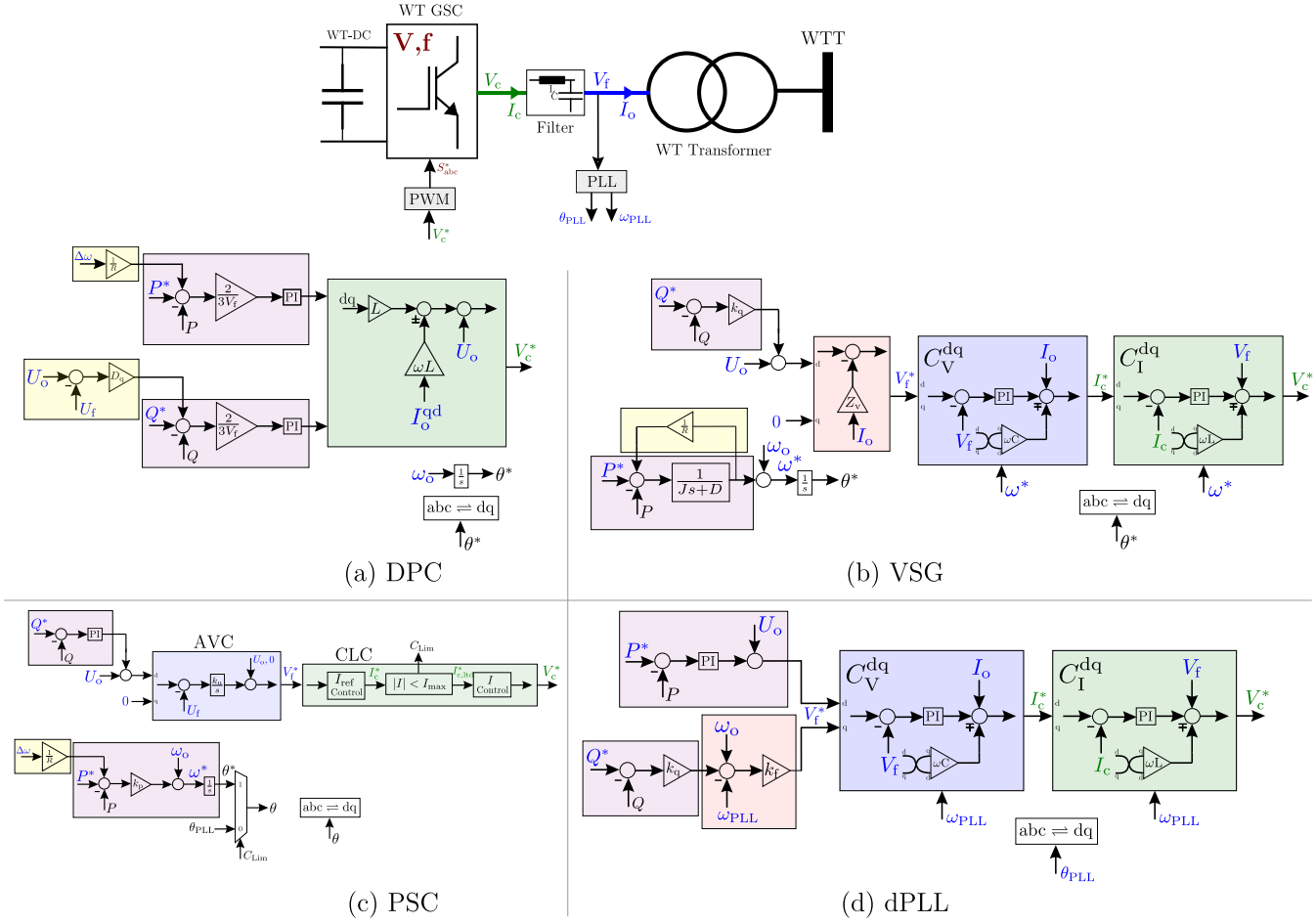

Figure 2. Control structure for (a) Direct Power Control (DPC), (b) Virtual Synchronous Generator (VSG), (c) Power Synchronous Control (PSC) and (d) Distributed-PLL based (dPLL) grid forming control strategies.

3.2.1 Virtual Synchronous Generator (VSG)

The VSG control structure implemented here is shown in figure 2(b), and is based on D'Arco et al. (2015). It uses standard cascaded voltage-current control with swing-equation (power-synchronization) for generating the frequency reference & synchronization angle and controlling real power. The reactive power controller based on Q-V droop is used to provide the voltage amplitude reference. Virtual impedance can also be added to reduce sensitivity to small grid disturbances by providing additional damping. Since a sufficiently high enough damping leads to a low inherent steady-state $\frac{\Delta P}{\Delta f}|_{\infty}$ droop, an external *secondary* virtual governor f-P droop is needed to mimic the traditional 3-5% SG speed droop characteristic.

https://doi.org/10.5194/wes-2020-34
Preprint. Discussion started: 17 March 2020

eawe european academy of wind energy
Open Access WIND ENERGY SCIENCE DISCUSSIONS

3.2.2 Power Synchronous Control (PSC)

The PSC control structure, explained in Zhang et al. (2010), is shown in figure 2(c). Here also power synchronization is used just like in VSG, however unlike the swing equation where the power difference drives the rotor speed dynamics which is then changed to electrical angle i.e. double integration for P-θ transfer function (equation 3), the the PSC Loop (PSL) directly gets the phase angle by a single integration of the power difference, as given by the equation 4. Due to 1 less integrator, PSC has higher stability margin, however due to 0 inherent steady-state droop, outer droops are needed for paralleling multiple grid forming units. Moreover, no virtual inertia or damping is present due to absence of rotor dynamics.

$$P_{\mathrm{m}} - P_{\mathrm{e}} = J\omega\frac{\mathrm{d}\omega}{\mathrm{d}t},\ \frac{\mathrm{d}\omega}{\mathrm{d}t} = \theta \Longleftarrow \text{ Swing Equation} \tag{3}$$

$$J\frac{\mathrm{d}\Delta\theta}{\mathrm{d}t} = k_{\mathrm{P}}(P_{\mathrm{m}} - P_{\mathrm{e}}) \Longleftarrow \text{PSL} \tag{4}$$

For the AC Voltage Controller (AVC), an emulation of the exciter of a SM is used except that integral control is used instead of the traditional proportional control, to supress high-frequency disturbances. Analysis by Zhang et al. (2010) shows that the open loop $\frac{\Delta P(s)}{\Delta\theta(s)}$ transfer function has a right half plane (RHP) zero meaning extra time delay & *non-minimum phase system* type response. Additionally, the RHP zero moves closer to origin at higher converter-voltages & load-angles leading to lower bandwidth and lesser phase margin. Finally, grid-frequency resonant poles (for low resistance grids) are also present that need to be damped out, for which the voltage control is governed by equation 5, where $H_{\mathrm{HP}}(s)$ is a high-pass filter used for resonance damping, as it is effectively a virtual resistor at high frequencies. Lastly, a Current Limitation Controller (CLC), employing equations 7 & 8, is used, which in *normal* mode simplifies to equation 5, but in *fault* mode limits the current output of the converter to $I_{\max}$ and generates a selector signal C_{Lim} to disable the PSL and switch to conventional PLL-based synchronization. The PSC has demonstrated strong performance in weak networks.

$$\boldsymbol{v}_{\mathrm{C}}^{*} = V_0 - H_{\mathrm{HP}}(s)\mathbf{i}_{\mathrm{C}} \Longleftarrow \text{ Voltage control} \tag{5}$$

$$H_{\mathrm{HP}}(s) = \frac{k_{\mathrm{v}}s}{s+\alpha_{\mathrm{v}}} \Longleftarrow \text{ High pass filter} \tag{6}$$

$$\boldsymbol{i}_{\mathrm{C}}^{*} = \frac{1}{\alpha L_{\mathrm{C}}}[V_0 - \boldsymbol{v}_{\mathrm{F}} - j\omega L_{\mathrm{C}}\boldsymbol{i}_{\mathrm{C}} - H_{\mathrm{HP}}(s)\boldsymbol{i}_{\mathrm{C}}] + \boldsymbol{i}_{\mathrm{C}} \Longleftarrow \text{ Current reference control} \tag{7}$$

$$\boldsymbol{v}_{\mathrm{C}}^{*} = \alpha L_{\mathrm{C}}(\boldsymbol{i}_{\mathrm{C}}^{*} - \boldsymbol{i}_{\mathrm{C}}) + j\omega L_{\mathrm{C}}\boldsymbol{i}_{\mathrm{C}} + \boldsymbol{v}_{\mathrm{F}} \Longleftarrow \text{ Current control} \tag{8}$$

3.2.3 Distributed PLL-based (dPLL)

The dPLL control structure is based on Yu et al. (2018) and shown in figure 2(d). Originally developed for DRU-connected OWFs, the real power controller is used to generate the d-axis voltage reference as power flow is determined by offshore voltage, governed by equation 9, and a reactive power droop controller regulates frequency to share the DRU demanded Var. Instead of the conventional approach of setting the q-axis voltage reference to 0, since PLL output can be used as an indication

https://doi.org/10.5194/wes-2020-34
Preprint. Discussion started: 17 March 2020

of frequency deviation, a Frequency Control Loop characterized by equation 10, is embedded in the q-axis to use the output of the Q-f droop-controller.

$$V_{\mathrm{DC}} = 2\left(1.35V_{\mathrm{F}} - \frac{3}{\pi}XI_{\mathrm{DC}}\right) \tag{9}$$

$$V_{\mathrm{Fq}}^{*} = k_{\mathrm{f}}(f^{*} - f) \tag{10}$$

Yu et al. (2018) demonstrates frequency controllability with plug-and-play capability providing successful sequential start-up of the grid-forming WTs and automatic synchronization of the offline WTs during connection with minimal impact, to supply the Var required to energize transformers, filters and finally ramp up the offshore voltage and start delivering active power to onshore grid. However, only the start-up and synchronisation of an islanded OWF to an energized onshore synchronous power system via a DR-HVDC link is studied while the energisation of export cable and onshore converter, expected from a blackstart service provider, was not looked into.

3.2.4 Direct Power Control (DPC)

DPC was introduced by Noguchi et al. (1998) in which the instantaneous p & q are controlled without requiring AC voltage sensors, PLL or an inner current controller, by using a look-up table and hysteresis comparators on the power errors to select the optimum switching state of the converter. Since then it has undergone many enhancements to deliver improved performance like using space vector modulation for constant switching frequency, employing sliding mode control for robustness, model predictive control for the multivariable case, and grid voltage modulated DPC for good transient-response and steady-state performance in non-linear systems. The control structure shown in figure 2(a) is based on Gui et al. (2019), which derives a standard *dq*-axes current model from the well known *instantaneous pq theory* (Akagi et al., 2017) of the DPC model to eliminate the inner control loops.

4 Model Description

The schematic model of the system shown in figure 3 has been developed in PSCAD and is based on Sakamuri et al. (2019). It consists of a 400 MW grid-forming OWF connected to the onshore AC grid by means of a 200 km long 1200 MW $\pm$320 kV symmetrical monopole point-to-point (P2P) HVDC link, as shown in figure 3(a).

A Detailed Equivalent Model (DEM) of the Half-Bridge Modular Multilevel Converters (MMC) is used for both terminals of the VSC-HVDC link, which represents each sub-module (SM) as an equivalent circuit model, stacks them up in series, simplifies the whole circuit, solves the network using this model, and then converts back to the equivalent SMs. This gives a fast solution along with information about what happens inside the SMs. The offshore terminal (T2) MMC is controlled in grid-following mode since the offshore AC network voltage is formed by the grid-forming OWF, so the converter regulates the HVDC link voltage V_{DC} and reactive power injection Q_2 into T2. At the onshore terminal (T1), the MMC is controlled in grid-forming mode to regulate the onshore AC voltage magnitude V_1 & frequency f_1, in the scope of the blackstart case study

https://doi.org/10.5194/wes-2020-34
Preprint. Discussion started: 17 March 2020

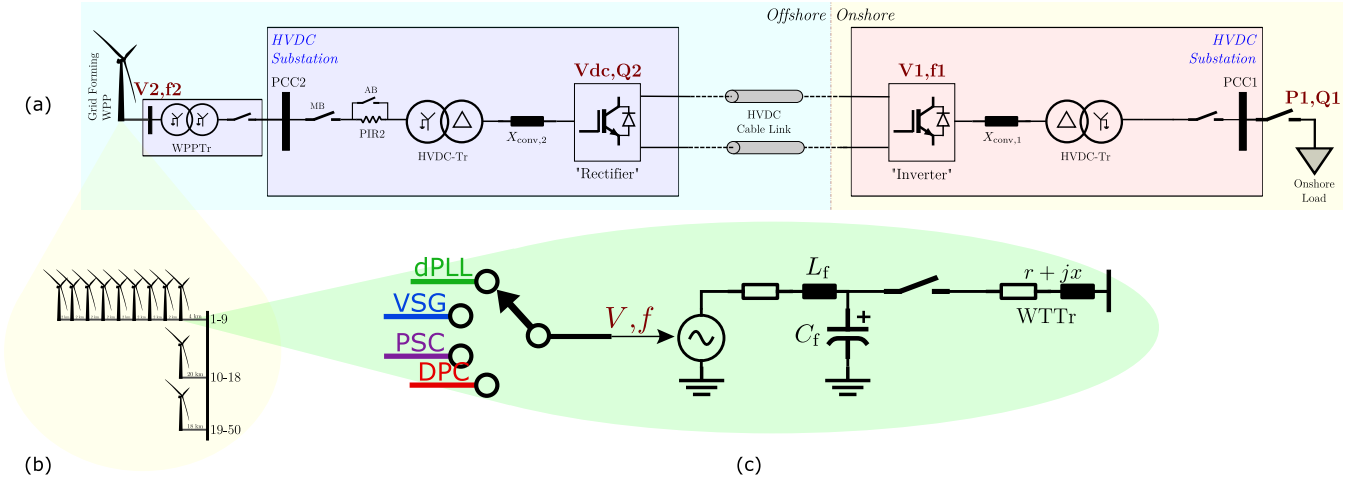

Figure 3. Schematic of the implemented PSCAD model of the system under study. This figure shows (a) the 2-Terminal P2P HVDC link, with grid-following offshore-MMC & grid-forming onshore-MMC (b) the partial aggregation used to model the OWF, and (c) the average model of the *grid-forming* WT-GSC implemented with 4 different control strategies operating in islanded mode.

performed in this paper. The MMC models used have standard HB-MMC inner control loops, such as cell voltage balancing and circulating current suppression, and the control structure for the V_{DC}-Q_2 (for T2) & V_1-f_1 (for T1) modes, can be seen in Sakamuri et al. (2019). Frequency dependent (phase) models in PSCAD are used for the HVDC export cable. The HVDC converter transformers models include magnetic characteristics such as saturation and inrush current. Finally, a Pre-Insertion Resistor (PIR) that is bypassed after a Pre-Insertion Time (PIT) by using coordinated Main & Auxilary Breakers (MB & AB), is used for limiting the transient magnetic-inrush current peak during hard-switching energization of the HVDC transformer.

The OWF consists of 50 Type-4 (fully-rated PEC interface) 8 MW WTs, as a *partially-aggregated* model shown in figure 3(b), based on Muljadi et al. (2008). It consists of 9 individual WT_{1-9} models on the first string, the second string with WT_{10-18} aggregated into a 72 MW WT model, and the remaining 32 WT_{19-50} aggregated into one 256 MW model. Coupled π-section models are used for the 66 kV array cables and magnetic detailed model (inrush & saturation) is used for the $66|155$ kV offshore WPP transformer. Lastly, the WT is modelled as a grid-forming unit operating in islanded mode, and so the Grid-Side Converter (GSC) is modelled as a voltage source (average model) controlled by the 4 different grid-forming strategies, viz. VSG, PSC, dPLL & DPC, that are explained in section 3.2. This is shown in figure 3(c).

4.1 Limitations & Assumptions

The model described above has certain limitations. Firstly, the WT Rotor-Side Converter (RSC) & changes to the turbine controller that are required for grid-forming operation, have not been modelled. In conventional grid-following operation of the WT, the RSC is controlled to extract maximum power from the generator while the GSC maintains power balance to control the DC link voltage of the back-to-back PEC interface of the WT and the reactive power output at the AC terminal.

https://doi.org/10.5194/wes-2020-34
Preprint. Discussion started: 17 March 2020

eawe european academy of wind energy
Open Access WIND ENERGY SCIENCE DISCUSSIONS

Table 1. Energization Sequence

Stage	Time [s]	Events
1	0	WTs energized simultaneously and operate in grid-forming mode.
2	1.3	WPP begins offshore grid-forming at PCC-2 and
		MB is closed to insert PIR for energizing the offshore transformer and pre-charging the offshore MMC cells.
	1.6	PIR is bypassed after PIT (= 0.3s) by closing AB.
3	2.1	Offshore MMC is de-blocked to control the DC voltage; HVDC link is energized
4	2.5	(a) Controlled pre-charging of onshore MMC's upper arm cells with lower arm blocked.
	2.8	(b) Controlled pre-charging of onshore MMC's lower arm cells with upper arm blocked.
	3.1	(c) Controlled pre-charging of onshore MMC finished; both arms blocked.
5	3.3	Onshore MMC is de-blocked to control voltage & frequency; Onshore AC PCC-1 is energized.
6	4	Onshore 30 MW block load is connected.

However, in grid-forming mode, the GSC can not control the DC link & reactive power anymore and the required generator torque & real power is set by the AC-load, not the turbine controller, which now has to regulate the speed using the pitch controller (and especially avoid overspeeding during low AC-load & high winds). Hence, the RSC control requires changes to be able to maintain the DC link voltage constant by ensuring real power balance (Pérez et al., 2019). Since the WT rotor & DC-link dynamics are outside the scope of this study, the model assumes a constant WT-DC link voltage. Additionally, since an average voltage source model of the GSC is used for the purpose of reducing simulation time, switching transients and their related issues like voltage surges or TOVs are not modelled. Moreover, the WT transformer is modelled as a pure electrical impedance $r + jx$ without any magnetic characteristics as it can be *soft-started* along with the WT voltage ramp-up, to avoid magnetic inrush & saturation effects. Secondly, for this study, although power sharing between the WTs inside the WPP has been controlled by including the outer power control loops, the WTs are started-up *simultaneously* as opposed to a more realistic *sequential* energization (eg. Yu et al. (2018)), as the study mainly focuses on the capabilities of the grid-forming OWF to provide blackstart services to the onshore grid while dealing with offshore network transients due to energization of the large converter transformer, HVDC converters and export cable, in a controlled manner. This puts any synchronization dynamics of multiple grid-forming PEC interfaced WTs out of the scope of this study. Additionally, substation load has not been modelled here because it is negligible with respect to onshore load.

5 Simulation Results

In this section, the results of the dynamic simulations performed in PSCAD are presented. The energization sequence, events of which are described in detail in table 1, is based on Sakamuri et al. (2019), but includes an extra stage of *DC-side controlled pre-charging* of the onshore MMC cells and the outer $C_{\mathrm{P,Q}}$ control loops for real & reactive power sharing amongst the WTs

https://doi.org/10.5194/wes-2020-34
Preprint. Discussion started: 17 March 2020

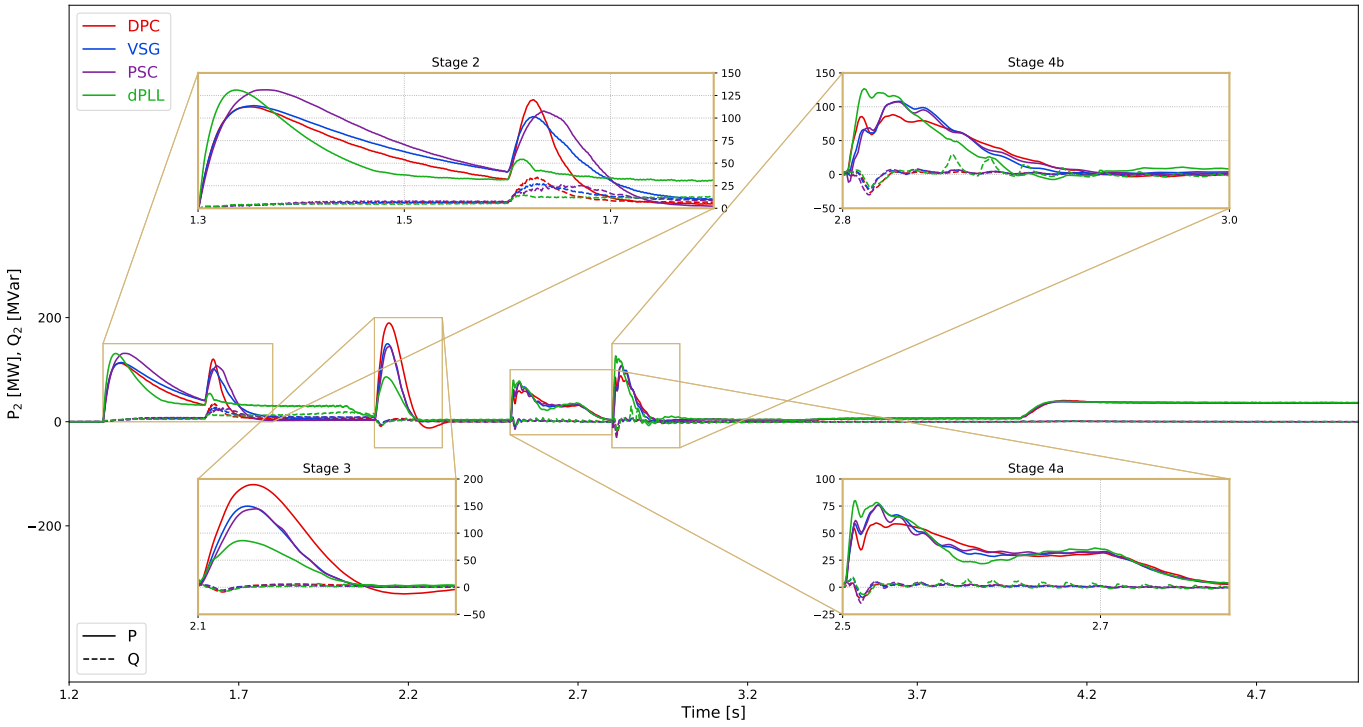

Figure 4. Real (solid line) & reactive (dotted line) power outpu of the offshore WPP with zoomed insets to show transients in selected stages of the energization sequence.

inside the WPP. The entire sequence is simulated, however the main focus is on testing the characteristics of the different control strategies in enabling the OWF to deal with the energization transients and so we focus on the real & reactive power outputs of the WPP, and with the voltage & frequency at the offshore PCC-2. *Hard-switching* is used here despite the advantages of *soft-start* energization, as the former is more demanding on the grid-forming OWF in terms of the transients (eg. TOV, oscillations) linked to energization of transformer, cable and HVDC link.

Figure 4 shows the waveforms for the real & reactive power outputs of the WPP during the different stages of the energization sequence. Since the grid-forming offshore WPP is operating in islanded mode, the real & reactive power demand is set by the load, which depends on the particular stage of energization. For stage 2, it is the Var required for magnetic energization of the offshore transformer and *AC-side* pre-charging of the offshore MMC cells. A PIR is inserted for PIT to limit the inrush peak. In stage 3, power is required to energize the HVDC cable when the offshore MMC is de-blocked to control the HVDC link voltage, while in stage 4, the *DC-side* pre-charging of the onshore MMC cells draws power from the OWF to maintain the energy balance on the HVDC link. Finally, the OWF supplies power to match the onshore block load in stage 6. Since the scope of this study is to focus on the offshore wind farm behaviour as a voltage source during the different stages of energization, the waveforms for the voltage & frequency at the offshore PCC-2 are presented in figures 5 & 6, respectively.

https://doi.org/10.5194/wes-2020-34
Preprint. Discussion started: 17 March 2020

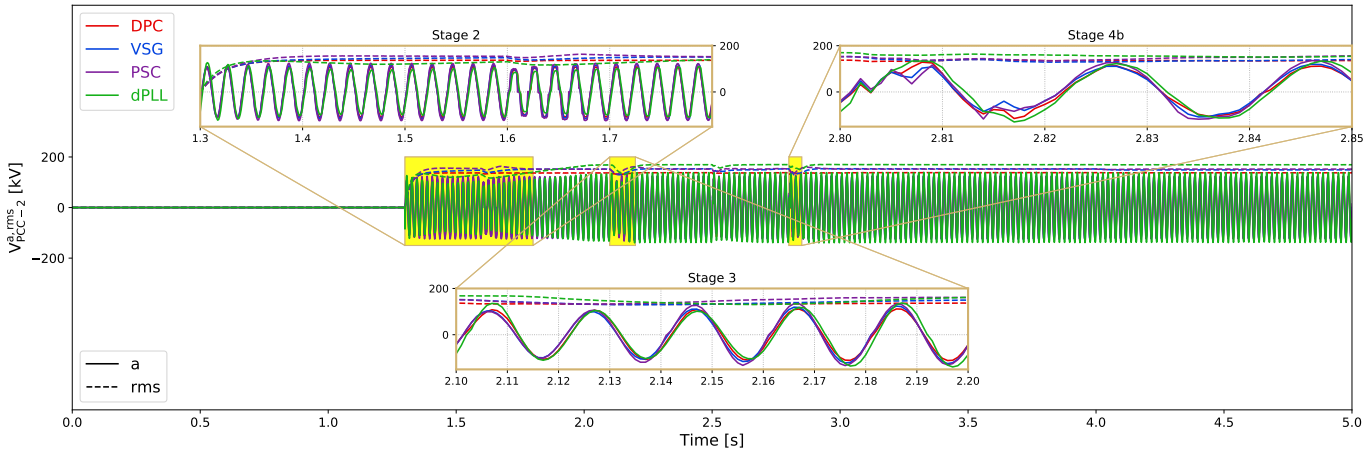

Figure 5. Voltage at offshore PCC-2 with zoomed insets to show transients in selected stages of the energization sequence.

The grid-forming WPP, controlled as a voltage source, has different characteristics based on the control method used. DPC is the most straightforward control technique with *direct* voltage and frequency control, without any inner loops, and doesn't have any electro-mechanical characteristics like inertia or damping. Thus it has the highest frequency swing, as can be seen from figure 6, along with highest transient peaks visible in the zoomed insets of the power waveform in figure 4, mainly stages 2 & 3. Comparatively, VSG has a lower frequency dip due to inertia emulation in its power controller, along with lower transient power peaks due to damping provided by virtual impedance. On the other hand, PSC has a higher frequency swing than VSG due to absence of inertia emulation, but the damping provided by $H_{\mathrm{HP}}(s)$ in the AVC reduces the transient power peak compared to DPC, visible in stages 2 & 3 of figure 4. However, the RHP zero in the PSC leads to an inherent delay that can be seen especially, from the shifted frequency nadir after the 2.8s event in stage 4 of figure 6 and the shifted power peak after the 1.6s event in stage 2 of figure 4. Additionally, the non-minimum phase system type behaviour of the PSC due to its RHP zero is also evident from the frequency rise as opposed to dip for other 3 methods, at the 1.6s event in stage 2 of figure 6. Contrary to the *power-synchronization based* VSG & PSC methods, the frequency swing in dPLL is lowest in all stages 2-6 with no overshoot in stage 1, as is clear from the figure 6, due to the frequency controllability of the *PLL-based* frequency control loop, which also provides damping and reduces the transient power peak, seen especially after the 1.6s event in stage 2 and stage 3 in fgure 4. However, after the 1.3s event in stage 2 in figure 4 the transient power peak for dPLL is higest during energization of the transformer with a PIR. This is because the dPLL is a voltage source controlled with Q-f, P-V coupling which not only leads to a drop in frequency when Var is demanded by the magnetic reactance of the transformer, but also causes a significantly higher distortion in voltage, compared to the other 3 methods, as shown in stage 2 of figure 5, due to the PIR reducing the decoupling, to which the dPLL controlled WPP reacts with a surge in power output.

It is clear from the PQ waveforms shown in figure 4 that there are some differences in the transient behaviour of the 4 control strategies, despite having an overall similar profile. The zoomed insets for the different stages in the V waveform in figure 5 show that the OWF with the 4 different grid-forming controls can successfully energize the transformer, cables &

https://doi.org/10.5194/wes-2020-34
Preprint. Discussion started: 17 March 2020

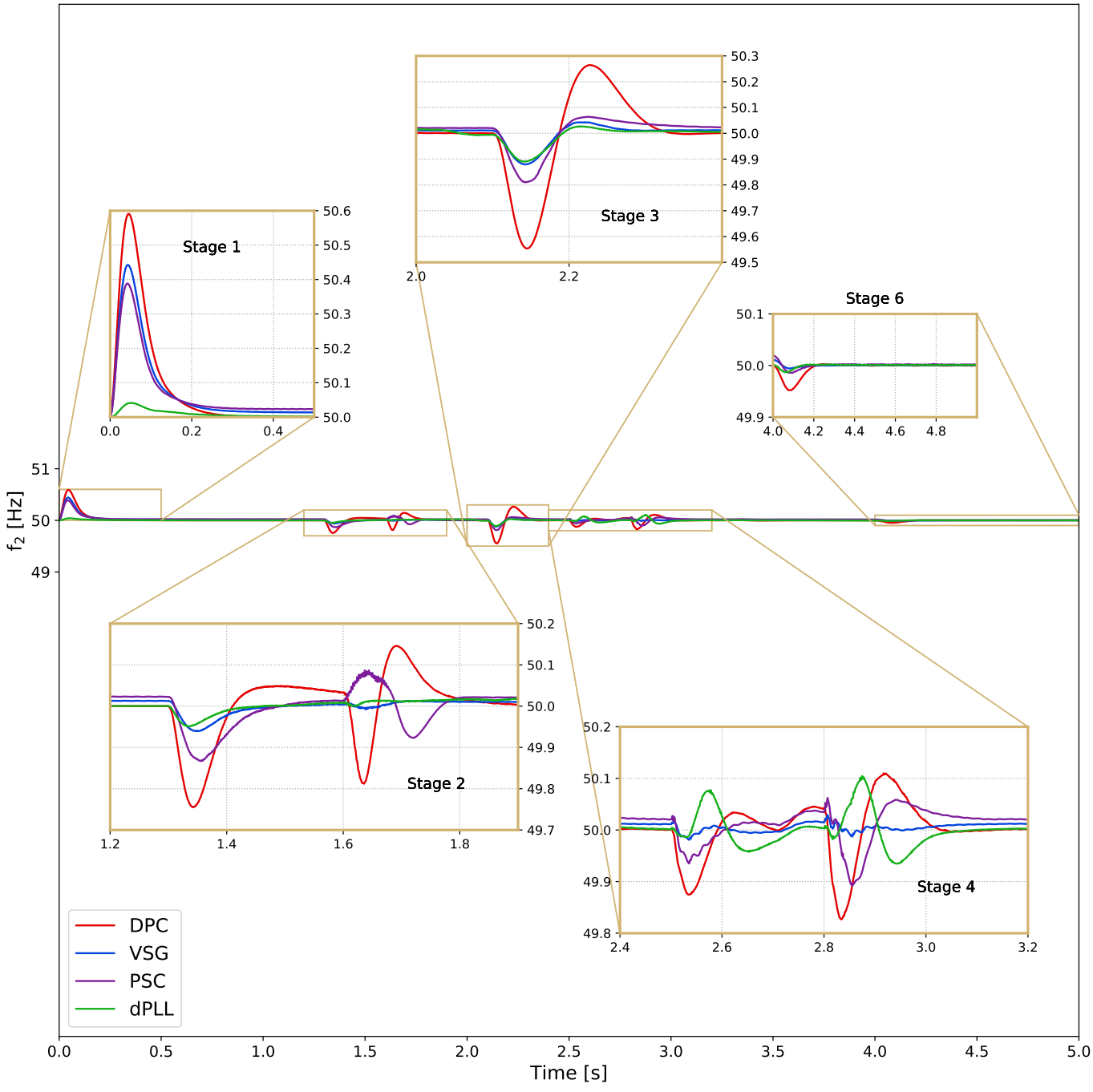

Figure 6. Frequency at offshore PCC-2 with zoomed insets to show transients in the different stages of the energization sequence.

https://doi.org/10.5194/wes-2020-34
Preprint. Discussion started: 17 March 2020

eawe european academy of wind energy
Open Access WIND ENERGY SCIENCE DISCUSSIONS

Table 2. Summary of the differences in transient behaviour of the different grid-forming control methods; + good (low amplitude), − bad (high amplitude).

Control	Frequency Swing	Power Peak	Remark
DPC	−	−	No electro-mechanical characteristics
PSC	−	−	Non-minimum phase, RHP zero
VSG	+	+	Inertia, Damping, Inherent droop
dPLL	++	++	PLL-enhanced frequency control

MMC cells and supply the onshore load, while maintaining a stable voltage at the offshore PCC-2, with only minor distortions during stages 2-4 that are recovered fast by the grid-forming controls. However, significant difference difference can be seen in the frequency transients in figure 6 which also demonstrates the characteristics of the different control methods. This is summarized in table 2.

6 Conclusions

Recent tests on HVDC interconnectors like SK-4 and NEMO link have shown that VSC-HVDC can be used for blackstart services in a *top-down* restoration strategy. This makes VSC-HVDC connected offshore wind farms promising candidates for providing blackstart and islanding operation capabilities, as the conventional large thermal power plants are being phased out and wind farms grow bigger, to meet the decarbonization aims. This paper presents an overview of the different strategies for the participation of offshore wind in a traditional *bottom-up* power system restoration procedure and focuses on *grid-forming* as the main control change required to enable blackstart and islanding services from wind turbines, facilitate their earlier participation and minimize the dependence on auxiliary diesel generators. The overall structure of grid forming control has been explained with the constituent functional blocks, along with conceptual explanation of 4 different techniques viz. VSG, PSC, dPLL and DPC. These methods were then tested in a study of the blackstart of onshore load by an HVDC-connected offshore wind farm, focusing on transients due to energization of transformers, cables, MMC cells and HVDC link. The simulation results demonstrate that all the 4 methods are able to deal with the energization transients in a controlled manner while maintaining stability of voltage and frequency at the offshore terminal. However, differences in their transient behaviours were observed and are summarised in table 2. The DPC & PSC have high frequency swing & transient power peaks, with the latter additionally having non-minimum phase behaviour. Contrarily, VSG & dPLL show superior performance but need further investigation, especially in regards to offshore & harmonic load sharing, synchronization transients during sequential energization of wind turbines inside the wind farm, and the effect of blackstart and islanded operation on rotor & turbine DC link dynamics, before wind turbines can be deemed blackstart-*able*.

https://doi.org/10.5194/wes-2020-34
Preprint. Discussion started: 17 March 2020

eawe european academy of wind energy
Open Access WIND ENERGY SCIENCE DISCUSSIONS

Code and data availability. Inquiries about and requests for access to the simulation models used in this study should be directed to the authors.

Appendix A: Parameters

Table A1. Main circuit parameters of the model [T2 - offshore, T1 - onshore, X_{L} - leakage reactance].

Parameters	**Values**
WT rating	8 MW, 66 kV
WT GSC Filter	$L_{\mathrm{f}} = 10\%$, $C_{\mathrm{f}} = 5\%$
WT transformer	$R = 1\%$, $X_{\mathrm{L}} = 1\%$
WPP rating	400 MW
WPP transformer	$66\vert155$ kV, $X_{\mathrm{L}} = 12\%$
HVDC transformers	1000 MVA, $X_{\mathrm{L}} = 15\%$
	T2: $155\vert390$ kV, T1: $390\vert400$ kV
PIR, PIT	120 Ω, 0.3 s
HVDC link rating	±320 kV, 1200 MW, 200 km
MMC DEM	1000 MVA, 225 submodules per arm
Onshore load	30 MW

Author contributions. JS designed the simulation for the case study. AJ and JS implemented the models and carried out the simulations. JS and NC analysed the results. AJ prepared the manuscript with contributions from JS and NC.

Competing interests. The authors declare that no competing interests are present.

Acknowledgements. This work is part of the InnoDC project that has received funding from the European Union's Horizon 2020 research and innovation programme under the Marie Skłodowska-Curie grant agreement No 765585.

https://doi.org/10.5194/wes-2020-34
Preprint. Discussion started: 17 March 2020

References

Akagi, H., Watanabe, E. H., and Aredes, M.: Instantaneous Power Theory and Applications to Power Conditioning, John Wiley & Sons, Inc., Hoboken, New Jersey, 2 edn., 2017.

Aktarujjaman, M., Kashem, M., Negnevitsky, M., and Ledwich, G.: Black start with DFIG based distributed generation after major emergencies, in: 2006 IEEE International Conference on Power Electronic, Drives and Energy Systems, pp. 1–6, 2006.

Andersen, B. and Xu, L.: Hybrid HVDC System for Power Transmission to Island Networks, IEEE Transactions on Power Delivery, 19, 1884–1890, 2004.

Arbab-Zavar, B., Palacios-Garcia, E. J., Vasquez, J. C., and Guerrero, J. M.: Smart Inverters for Microgrid Applications: A Review, Energies, 12, 840, 2019.

Arghir, C., Jouini, T., and Dörfler, F.: Grid-forming Control for Power Converters based on Matching of Synchronous Machines, Automatica, 95, 273–282, 2018.

Aten, M., Shanahan, R., Mosallat, F., and Wijesinghe, S.: Dynamic Simulations of a Black Starting Offshore Wind Farm Using Grid Forming Converters, in: 18th Wind Integration Workshop, Energynautics GmbH, Dublin, 2019.

Australian Energy Market Operator: Black system, South Australia, 28 September 2016 - Final Report, 2017.

Bahrman, M. and Bjorklund, P.-E.: The New Black Start: System Restoration with Help from Voltage-Sourced Converters, IEEE Power and Energy Magazine, 12, 44–53, 2014.

Beck, H. P. and Hesse, R.: Virtual synchronous machine, in: 9th International Conference on Electrical Power Quality and Utilisation, EPQU, Barcelona, 2007.

Becker, H., Naranovich, A., Hennig, T., Akbulut, A., Mende, D., Stock, S., and Hofmann, L.: System restoration using VSC-HVDC connected offshore wind power plant as black-start unit, in: 2017 19th European Conference on Power Electronics and Applications (EPE'17 ECCE Europe), 2017.

Blasco-Gimenez, R., Añó-Villalba, S., Rodríguez-D'Derlée, J., Morant, F., and Bernal-Perez, S.: Distributed voltage and frequency control of offshore wind farms connected with a diode-based HVdc link, IEEE Transactions on Power Electronics, 25, 3095–3105, 2010.

Cai, L., Karaagac, U., and Mahseredjian, J.: Simulation of Startup Sequence of an Offshore Wind Farm with MMC-HVDC Grid Connection, IEEE Transactions on Power Delivery, 32, 638–646, 2017.

Chen, Z., Guerrero, J. M., and Blaabjerg, F.: A Review of the State of the Art of Power Electronics for Wind Turbines, IEEE Transactions on Power Electronics, 24, 1859–1875, 2009.

D'Arco, S. and Suul, J. A.: Virtual synchronous machines - Classification of implementations and analysis of equivalence to droop controllers for microgrids, in: 2013 IEEE PES PowerTech, Grenoble, 2013.

D'Arco, S., Suul, J. A., and Fosso, O. B.: A Virtual Synchronous Machine implementation for distributed control of power converters in SmartGrids, Electric Power Systems Research, 122, 180–197, 2015.

De Boeck, S., Van Hertem, D., Das, K., Sørensen, P. E., Trovato, V., Turunen, J., and Halat, M.: Review of Defence Plans in Europe: Current Status, Strengths and Opportunities, CIGRE Transactions on Science & Engineering, 5, 6–16, 2016.

El-Zonkoly, A.: Integration of wind power for optimal power system black-start restoration, Turkish Journal of Electrical Engineering & Computer Sciences, 23, 1853–1866, 2015.

Elia: Study on the Review of the Black Start Ancillary Services, 2018.

https://doi.org/10.5194/wes-2020-34
Preprint. Discussion started: 17 March 2020

Erlich, I., Shewarega, F., Feltes, C., Koch, F. W., and Fortmann, J.: Offshore wind power generation technologies, Proceedings of the IEEE, 101, 891–905, 2013.

Erlich, I., Korai, A., Neumann, T., Koochack Zadeh, M., Vogt, S., Buchhagen, C., Rauscher, C., Menze, A., and Jung, J.: New Control of Wind Turbines Ensuring Stable and Secure Operation Following Islanding of Wind Farms, IEEE Transactions on Energy Conversion, 32, 1263–1271, 2017.

European Parliament and Council of the European Union: Directive (EU) 2018/2001 of the European Parliament and of the Council on the promotion of the use of energy from renewable sources (recast), Official Journal of the European Union, L 328, 82–209, 2018.

Göksu, Ö., Saborío-Romano, O., Cutululis, N. A., and Sørensen, P.: Black Start and Island Operation Capabilities of Wind Power Plants, in: 16th Wind Integration Workshop, Berlin, Germany, 2017.

Green, T. C. and Prodanović, M.: Control of inverter-based micro-grids, Electric Power Systems Research, 77, 1204–1213, https://doi.org/10.1016/j.epsr.2006.08.017, 2007.

Guerrero, J. M., Vasquez, J. C., Matas, J., De Vicuña, L. G., and Castilla, M.: Hierarchical control of droop-controlled AC and DC microgrids - A general approach toward standardization, IEEE Transactions on Industrial Electronics, 58, 158–172, 2011.

Gui, Y., Wang, X., and Blaabjerg, F.: Vector Current Control Derived from Direct Power Control for Grid-Connected Inverters, IEEE Transactions on Power Electronics, 34, 9224–9235, 2019.

Heising, C., Meyer, D., Hennig, T., Vennemann, K., Deiml, G., Winter, W., Wrede, H., Lehner, J., Wenig, S., Johannes Weidner, S. K., and Fortmann, J.: Need for Grid-Forming Converter-Control in Future System-Split Scenarios, in: 18th Wind Integration Workshop, Energynautics GmbH, Dublin, 2019.

Jain, A., Das, K., Göksu, Ö., and Cutululis, N. A.: Control Solutions for Blackstart Capability and Islanding Operation of Offshore Wind Power Plants, in: Proceedings of the 17th International Wind Integration workshop, Energynautics GmbH, 2018.

Jain, A., Sakamuri, J. N., Das, K., Göksu, Ö., and Cutululis, N. A.: Functional Requirements for Blackstart and Power System Restoration from Wind Power Plants, in: 2nd International Conference on Large-Scale Grid Integration of Renewable Energy in India, Energynautics GmbH, New Delhi, 2019.

Jiang-Hafner, Y., Duchen, H., Karlsson, M., Ronstrom, L., and Abrahamsson, B.: HVDC with voltage source converters - A powerful standby black start facility, in: Transmission and Distribution Exposition Conference: 2008 IEEE PES Powering Toward the Future, PIMS 2008, 2008.

Johnson, B., Rodriguez, M., Sinha, M., and Dhople, S.: Comparison of virtual oscillator and droop control, in: 2017 IEEE 18th Workshop on Control and Modeling for Power Electronics (COMPEL), IEEE, 2017.

Martínez-Turégano, J., Año-Villalba, S., Bernal-Pérez, S., Peña, R., and Blasco-Gimenez, R.: Mixed Grid-Forming and Grid-Following Wind Power Plants for Black Start Operation, in: 17th International Wind Integration Workshop, Energynautics GmbH, Stockholm, 2018.

Muljadi, E., Pasupulati, S., Ellis, A., and Kosterov, D.: Method of equivalencing for a large wind power plant with multiple turbine representation, in: 2008 IEEE Power and Energy Society General Meeting - Conversion and Delivery of Electrical Energy in the 21st Century, 2008.

National Grid: Technical Report on the events of 9 August 2019, 2019a.

National Grid: Black Start from Non - Traditional Generation Technologies, 2019b.

Noguchi, T., Tomiki, H., Kondo, S., and Takahashi, I.: Direct power control of PWM converter without power-source voltage sensors, IEEE Transactions on Industry Applications, 34, 473–479, 1998.

https://doi.org/10.5194/wes-2020-34
Preprint. Discussion started: 17 March 2020

Pérez, A. N. F., Sun, Y., Burstein, A. W., Harson, A., and Tang, B.: Co-simulation Hardware in the Loop Test bench for a Wind Turbine: Validation of a wind turbine black start capability, in: 18th Wind Integration Workshop, Energynautics GmbH, Dublin, 2019.

Pogaku, N., Prodanović, M., and Green, T. C.: Modeling, analysis and testing of autonomous operation of an inverter-based microgrid, IEEE Transactions on Power Electronics, 22, 613–625, 2007.

Qing-Chang Zhong, Phi-Long Nguyen, Zhenyu Ma, and Wanxing Sheng: Self-Synchronized Synchronverters: Inverters Without a Dedicated Synchronization Unit, IEEE Transactions on Power Electronics, 29, 617–630, 2014.

Rocabert, J., Luna, A., Blaabjerg, F., and Rodriguez, P.: Control of Power Converters in AC Microgrids, IEEE Transactions on Power Electronics, 27, 4734–4749, 2012.

Sakamuri, J. N., Göksu, Ö., Bidadfar, A., Saborío-Romano, O., Jain, A., and Cutululis, N. A.: Black Start by HVdc-connected Offshore Wind Power Plants, in: IECON 2019 - 45th Annual Conference of the IEEE Industrial Electronics Society, Lisbon, 2019.

Sarkar, M. N. I., Meegahapola, L. G., and Datta, M.: Reactive Power Management in Renewable Rich Power Grids: A Review of Grid-Codes, Renewable Generators, Support Devices, Control Strategies and Optimization Algorithms, IEEE Access, 6, 41 458–41 489, 2018.

Schyvens, T.: Interactions Between Transmission System Connected Converters, in: IEEE Power and Energy Society General Meeting, Atlanta, GA, 2019.

Seca, L., Costa, H., Moreira, C. L., and Pecas Lopes, J. A.: An innovative strategy for power system restoration using utility scale wind parks, in: Proceedings of IREP Symposium: Bulk Power System Dynamics and Control - IX Optimization, Security and Control of the Emerging Power Grid, IREP 2013, 2013.

Sørensen, T. B., Kwon, J. B., and Jørgensen, J. M.: A live black start test of an HVAC network using soft start capability of a voltage source HVDC converter, in: CIGRE 2019 Aalborg Symposium, 2019.

Tavner, P.: Offshore Wind Turbines: Reliability, availability and maintenance, Institution Of Engineering & Technology (IET), 2012.

Tayyebi, A., Dörfler, F., Miletic, Z., Kupzog, F., and Hribernik, W.: Grid-Forming Converters – Inevitability, Control Strategies and Challenges in Future Grids Application, in: CIRED Workshop 2018, Ljubljana, 2018.

van Wesenbeeck, M. P., de Haan, S. W., Varela, P., and Visscher, K.: Grid tied converter with virtual kinetic storage, in: 2009 IEEE PowerTech Conference, pp. 1–7, Bucharest, 2009.

Yu, L., Li, R., and Xu, L.: Distributed PLL-based Control of Offshore Wind Turbine Connected with Diode-Rectifier based HVDC Systems, IEEE Transactions on Power Delivery, 33, 1328–1336, 2018.

Zeni, L., Hesselbaek, B., Sorensen, P. E., Hansen, A. D., and Kjaer, P. C.: Control of VSC-HVDC in offshore AC islands with wind power plants: Comparison of two alternatives, 2015 IEEE PowerTech Conference, 2015.

Zhang, L., Harnefors, L., and Nee, H. P.: Power-synchronization control of grid-connected voltage-source converters, IEEE Transactions on Power Systems, 25, 809–820, 2010.

Zhong, Q.-c. and Weiss, G.: Static Synchronous Generators for Distributed Generation and Renewable Energy, in: 2009 IEEE/PES Power Systems Conference and Exposition, pp. 1 – 6, 2009.

Zhu, L., Pan, Z., and Xu, G.: Black Start with DFIG-Based Wind Turbines Using Improved Virtual Synchronous Control, in: 2018 21st International Conference on Electrical Machines and Systems (ICEMS 2018), KIEE EMECS (KIEE Electrical Machinery and Energy Conversion Systems), 2018.